

$U(1) \times U(1)$ symmetry protected topological Order in Gutzwiller wave functions

Zheng-Xin Liu,^{1,2} Jia-Wei Mei,² Peng Ye,² and Xiao-Gang Wen^{3,2}

¹*Institute for Advanced Study, Tsinghua University, Beijing, 100084, P. R. China*

²*Perimeter Institute for Theoretical Physics, Waterloo, Ontario, N2L 2Y5 Canada*

³*Department of Physics, Massachusetts Institute of Technology, Cambridge, Massachusetts 02139, USA*

Gutzwiller projection is a way to construct many-body wave functions that could carry topological order or symmetry protected topological (SPT) order. However, an important issue is to determine whether a given Gutzwiller-projected wave functions (GWF) carries a non-trivial SPT order or not, and which SPT order is carried by the wavefunction. In this paper, we numerically study the SPT order in a $S = 1$ GWF on the Kagome lattice. Using the standard Monte Carlo method, we directly confirm that the GWF has (1) gapped bulk with short-range correlations, (2) a trivial topological order via non degenerate ground state, and zero topological entanglement entropy, (3) a non-trivial $U(1) \times U(1)$ SPT order via the Hall conductances of the protecting $U(1) \times U(1)$ symmetry, (4) symmetry protected gapless boundary. To our knowledge it is the first numerical evidence of continuous symmetry protected topological order in a Bosonic lattice system.

I. INTRODUCTION

Topological order^{1–3} was introduced to describe exotic quantum phases without symmetry breaking, such as fractional quantum Hall states^{4,5} or spin liquid sates.^{6,7} Opposite to Landau’s paradigm of symmetry breaking orders,^{8,9} topologically ordered phases can not be distinguished by local order parameters. It was shown that different topological orders differ by many-body entanglement.¹⁰ From this point of view, long-range entangled states are topologically ordered and are characterized by exotic properties, such as degeneracy of ground states on a torus, fractional excitations, non-zero topological entanglement entropy^{11,12}. On the other hand, a short range entangled state is trivial and can be adiabatically connected to a direct product state. However, if the system has a symmetry, the phase diagram will be enriched. Even short-range entangled states can belong to different phases, called symmetry protected topological (SPT) phases.^{13,14} Haldane phase^{15,16} and topological insulators^{17–21} are typical examples of phases that contain SPT orders. If the symmetry of a bosonic system is described by group G , then a large class of SPT phases in $d + 1$ -dimension can be constructed via group cohomology $\mathcal{H}^{d+1}(G, U(1))$ ²² or through nonlinear sigma models.^{22,23} In 2+1D, many SPT phases can also be understood through Chern-Simons effective theory.²⁴ Similar to quantum Hall states and topological insulators, the boundary of a 2+1D SPT phase must be gapless if the symmetry is not broken. For continuous symmetry groups such as $U(1)$ ^{22,24–27} or $SO(3)$,²⁸ different SPT phases can be distinguished by Hall conductance, which are quantized to 2. We like to remark that, before the recent studies of symmetry protected short-range entangled states with trivial topological order (*i.e.* the SPT states), some progresses were made on symmetry enriched long-range entangled states with non-trivial topological order, the so called symmetry enriched topological states,^{29–34} where the “fractionalized representation” of the symmetry, carried by topological excitations and described by

Projective Symmetry Group,^{29–31} played a key role.

Although it is believed that symmetry can enrich quantum phases of matter, it lacks simple lattice models to realize these nontrivial phases in spatial dimension higher than 1+1D. SPT phases for discrete symmetry groups were understood quite well, since the ground state wave functions and exactly solvable models (usually they are complicated and contain many-body interactions) for nontrivial SPT phases can be constructed.^{35,36} It is more challenging to realize continuous symmetry protected phases. A $U(1)$ symmetry protected nontrivial phase was reported in a continuous bose model,²⁷ and lattice models that may realize continuous (or combined) symmetry protected topological phases were proposed.^{37–40} In Ref. 38, the authors proposed projective construction of $SU(2)$ or $SO(3)$ SPT states. And lattice model Hamiltonians that may possibly stabilize SPT states are designed recently.⁴⁰

Using Gutzwiller-projected wave functions (GWF), we can construct different kinds of SPT states^{37,38}. In the present paper, we will numerically study a spin-1 state on the Kagome lattice constructed by Gutzwiller projected Chern Bands, which was firstly proposed in Ref. 37. We will show that this state is a $U(1) \times U(1)$ SPT state, where the two $U(1)$ groups correspond to S_z conservation and S_z^2 conservation, respectively. This SPT state has the following properties: it is gapped without conventional long range spin order; although it has non-zero spin Hall conductance, the $U(1) \times U(1)$ charge is not fractionalized; it has unique ground state and zero topological entanglement entropy; the boundary is gapless (if the symmetry is reserved) but can be gapped out by the perturbations that breaks the symmetry. As a comparison, we also study a $S = 1$ chiral spin liquid state⁴¹ (which are long-range entangled and contain intrinsic topological order), and show that its gapless edge state is robust against symmetry breaking perturbations. These properties of the Gutzwiller wave functions are directly confirmed numerically using the standard Monte Carlo method.

Remarkably, before projection, above two states are both chiral at mean field level, but after projection the

SPT state becomes non-chiral and the chiral spin liquid remains chiral.

The remaining part of this paper is organized as follows. In section II, we briefly review the projective construction for the GWF, especially for the $U(1) \times U(1)$ SPT state. In section III, we show that the GWF has (1) gapped short-range correlation in the bulk, (2) zero topological entanglement entropy and unique ground state, (3) nontrivial Hall conductance, (4) symmetry protected gapless boundary. Section IV is devoted to a summary.

II. GUTZWILLER CONSTRUCTION AND EFFECTIVE FIELD THEORY

A. Construction of Gutzwiller wave functions

We adopt the fermionic representation of $S = 1$ spin operators $\hat{S}_i^m = F_i^\dagger \mathcal{S}^m F_i$, where $F_i = (f_{1i}, f_{0i}, f_{-1i})^T$ and the spin state is described as $|m\rangle = f_m^\dagger |\text{vac}\rangle$ with $m = 1, 0, -1$.⁴²⁻⁴⁵ Here a particle number constraint $\hat{N}_i = f_{1i}^\dagger f_{1i} + f_{0i}^\dagger f_{0i} + f_{-1i}^\dagger f_{-1i} = 1$ should be imposed to ensure that the Hilbert space of fermions is the same as that of the spin. Notice that the spin operator is invariant under the following $U(1)$ gauge transformation $F_i \rightarrow F_i e^{i\varphi_i}$.

From the fermionic representation of $S = 1$ spin operators, one can construct trial spin wavefunctions for interacting spin-1 systems via Gutzwiller projected mean field ground states,

$$|\psi\rangle_{\text{spin}} = P_G |\text{MF}\rangle, \quad (1)$$

where $|\text{MF}\rangle$ is the ground state of some mean field Hamiltonian and the Gutzwiller projection P_G means only keeping the components of the mean field state that satisfy the particle number constraint $\hat{N}_i = 1$. Since the fermionic representation has a $U(1)$ gauge structure, the mean field state suffers from gauge fluctuations. Gutzwiller projection is a simple way to partially integrate out the gauge fluctuations to obtain trial spin wave functions. For example, in 1D Gutzwiller projected $SO(3)$ symmetric p -wave weak pairing states belong to a nontrivial SPT phase—the Haldane phase.⁴⁴

In this paper, we will consider the following pairing-free mean field Hamiltonian on the Kagome lattice,³⁷

$$H_{\text{mf}} = \sum_{ij} (t_{m,ij} f_{m,i}^\dagger f_{m,j} + h.c.) + \sum_i \lambda_i (N_i - 1), \quad (2)$$

where λ_i is the chemical potential and is uniform at mean field level. By tuning the phase of $t_{m,ij}$, we can set the Chern number of each species of fermions to be either 1 or -1 . For example, if we only consider nearest neighbor hopping and set the phase to be $e^{\pm i\pi/6}$ (see Fig. 1a & c), then Chern number for the lowest band is ± 1 . In the following discussion, we take the notation $|\mathcal{C}_1 \mathcal{C}_0 \mathcal{C}_{-1}\rangle$ as a mean field state and $P_G |\mathcal{C}_1 \mathcal{C}_0 \mathcal{C}_{-1}\rangle$ as the projected state, where the number $\mathcal{C}_m = \pm 1$ stands for the Chern number of the f_m species of fermion.

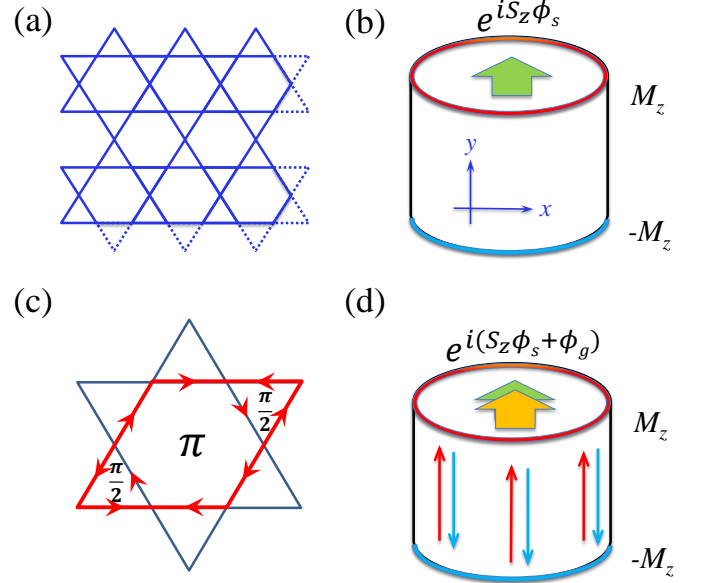


FIG. 1. (Color online) (a) The Kagome Lattice; (b) Laughlin's gauge invariant argument of the spin Hall conductance. Inserting a symmetry flux through the cylinder results in symmetry charge pumping from one edge to the other [M_z stands for S_z momentum according to the first $U(1)$ symmetry. Similarly, for the second $U(1)$ symmetry, the inserted flux should be $e^{S_z^2\phi_s}$ and then M_z stands for S_z^2 momentum]; (c) The mean field model on Kagome lattice with Chern number $\mathcal{C} = 1$. When hopping along the arrows the fermion gain a phase $e^{i\pi/6}$, when hopping against the arrow, the fermion gain a phase $e^{-i\pi/6}$; (d) Laughlin's argument at mean field level. An internal gauge flux should be introduced such that the induced particle number flow from one edge to the other exactly cancels that caused by the symmetry flux.

In above GWF, the particle numbers of three species of fermions are conserved respectively. This gives rise to two independent $U(1)$ spin symmetries, one generated by $\sum_i S_i^z$ and another by $\sum_i (S_i^z)^2$. The electric charge conservation is also a symmetry, but the charge degrees of freedom is frozen in the pure spin system. The projected state could be a topologically ordered state enriched by the $U(1) \times U(1)$ symmetry, or a SPT state protected by the $U(1) \times U(1)$ symmetry.

B. Effective field theory and physical response

We introduce three Chern-Simons field a_m to describe the current of the three species of fermions via $J_\mu^m = \frac{1}{2\pi} \varepsilon^{\mu\nu\lambda} \partial_\nu a_{m,\lambda}$. Then the mean field theory can be described by the Chern-Simons Lagrangian $\mathcal{L}_{\text{MF}} = -\frac{i}{4\pi} \sum_m \mathcal{C}_m^{-1} \varepsilon^{\mu\nu\lambda} a_{m,\mu} \partial_\nu a_{m,\lambda}$. Interactions can be restored if we couple the fermions to internal $U(1)$ gauge field \tilde{a}_μ (the fluctuations of λ_i and the phase fluctuations of $t_{m,ij}$ correspond to the temporal and spatial components of \tilde{a}_μ , respectively). Then the low energy effective theory for the spin system (or the Gutzwiller projected

states) is given as

$$\begin{aligned}\mathcal{L} &= -\frac{i}{4\pi} \sum_m \mathcal{C}_m^{-1} \varepsilon^{\mu\nu\lambda} a_{m\mu} \partial_\nu a_{m\lambda} + \frac{i}{2\pi} \sum_m \varepsilon^{\mu\nu\lambda} \tilde{a}_\mu \partial_\nu a_{m\lambda}, \\ &= -\frac{i}{4\pi} \varepsilon^{\mu\nu\lambda} a_\mu^T K \partial_\nu a_\lambda\end{aligned}\quad (3)$$

where $a_\mu = (a_{1\mu} \ a_{0\mu} \ a_{-1\mu} \ \tilde{a}_\mu)^T$ and

$$K = \begin{pmatrix} \mathcal{C}_1^{-1} & 0 & 0 & 1 \\ 0 & \mathcal{C}_0^{-1} & 0 & 1 \\ 0 & 0 & \mathcal{C}_{-1}^{-1} & 1 \\ 1 & 1 & 1 & 0 \end{pmatrix}.$$

Since \tilde{a}_μ can be considered as a Lagrangian multiplier, we can integrate it first and obtain an effective mutual Chern-Simons action described by a 2×2 K matrix (see Appendix C 2).³⁷

To detect the physical response, we couple the system with a probe fields A_μ^s (according to some symmetry) via

$$\mathcal{L}_{\text{probe}} = \frac{i}{2\pi} \varepsilon^{\mu\nu\lambda} A_\mu^s Q^T \partial_\nu a_\lambda,$$

where $Q = (q^s, 0)^T$, and q^s is the charge carried by the fermions according to the external probe field A_μ^s . For example, for the field $A_\mu^{S_z}$ that couple to the $U(1)$ charge $\sum_i S_i^z$, $q^{S_z} = (1, 0, -1)^T$; for the field $A_\mu^{S_z^2}$ that couple to the $U(1)$ charge $\sum_i (S_i^z)^2$, $q^{S_z^2} = (1, 0, 1)^T$; while for the electric-magnetic field that couple to the “electric” charge $\sum_i N_i$, $q^c = (1, 1, 1)$.

Integrating out a_μ we obtain the response theory

$$\mathcal{L}_{\text{res}} = \frac{i}{4\pi} \varepsilon^{\mu\nu\lambda} Q^T K^{-1} Q A_\mu^s \partial_\nu A_\lambda^s,$$

and the Hall conductance is

$$\sigma_H = \frac{1}{2\pi} Q^T K^{-1} Q.$$

C. Response mean field theory

When the system couples to an external probe field A_μ^s , the mean field theory should be modified accordingly. To get the correct response mean field Hamiltonian, we integrate out the matter field $a_{m\mu}$ to obtain the effective Lagrangian,

$$\mathcal{L}_{\text{eff}}(A, \tilde{a}) = \frac{i}{4\pi} \sum_m \mathcal{C}_m \varepsilon^{\mu\nu\lambda} (\tilde{a}_\mu + q_m A_\mu^s) \partial_\nu (\tilde{a}_\lambda + q_m A_\lambda^s).$$

The external field A_μ^s will induce a back ground internal gauge field \bar{a}_μ — the saddle point value of the \tilde{a} field which can be obtained from $\frac{\delta \mathcal{L}_{\text{eff}}(A^s, \tilde{a})}{\delta \tilde{a}_\mu} = 0$,⁴⁶

$$\bar{a}_\mu = -\frac{\sum_m \mathcal{C}_m q_m}{\sum_m \mathcal{C}_m} A_\mu^s. \quad (4)$$

Rewriting $\tilde{a}_\mu = \bar{a}_\mu + \delta\tilde{a}_\mu$, then we have,

$$\mathcal{L}_{\text{eff}}(A, \delta\tilde{a}) = \frac{i}{4\pi} \sum_m \varepsilon^{\mu\nu\lambda} \mathcal{C}_m [\tilde{q}_m^2 A_\mu \partial_\nu A_\lambda + \delta\tilde{a}_\mu \partial_\nu \delta\tilde{a}_\lambda],$$

where $\tilde{q}_m = q_m (1 - \frac{\sum_n q_n \mathcal{C}_n}{q_m \sum_n \mathcal{C}_n})$ is the screened charge. Integrating out $\delta\tilde{a}_\mu$ we obtain the response Lagrangian and the spin Hall conductance is given as $\sigma_H = \frac{1}{2\pi} \sum_m \mathcal{C}_m \tilde{q}_m^2$.

Noticing that the saddle point value \bar{a}_μ enters the mean field theory, thus the response mean field Hamiltonian with probing field A^s is given as

$$\begin{aligned}H_{\text{mf}}(A^s, \bar{a}) &= \sum_{m,ij} (t_{m,ij} e^{i\bar{a}_{ij} + iq_m A_{ij}} f_{m,i}^\dagger f_{m,j} + \text{h.c.}) \\ &\quad + \sum_i \lambda_i (N_i - 1),\end{aligned}\quad (5)$$

where \bar{a} is a function of A^s as given in (4). The physical quantities of the spin system can be measured from the Gutzwiller projected ground state of above mean field Hamiltonian.

The internal back ground gauge field \bar{a}_μ in above response mean field Hamiltonian is very important. Without \bar{a}_μ , GPW will give incorrect responses. To see why \bar{a}_μ is important, we consider the electromagnetic response as an example. It is known that a spin system is a Mott insulator having no charge response. However, if we barely couple the electromagnetic field A_μ^c to the fermions, after Gutzwiller projection the GPW still has dependence on A_μ^c , and the Chern-number for the GPW on the \mathbf{A}^c twisted-boundary-angle torus is nonzero. This seems to indicate that the system still have electromagnetic quantum Hall effect. This is obviously wrong. To obtain the correct response, we need to couple both A_μ^c and \bar{a}_μ to the fermions. Since $q^c = (1, 1, 1)^T$, from (4), $\bar{a}_\mu = -A_\mu^c$, so the mean field state and the projected state are independent on A_μ^c , which is consistent with the factor that the system is an insulator.

III. PHYSICAL PROPERTIES OF PROJECTED STATES

In this section, we will focus on the physical properties of the state $P_G|1-11\rangle$. From these properties we can judge if it is a SPT state or not. As a comparison, the chiral spin liquid (CSL) state $P_G|111\rangle$, which contain intrinsic topological order, is also studied.

A. Short range correlation in the bulk

We first check that the bulk is gapped without symmetry breaking. To this end, we calculate the spin-spin correlation $\langle S_r^z S_{r+x}^z \rangle$ and quadrupole-quadrupole correlation $\langle Q_r^x Q_{r+x}^x \rangle$ where $Q^x = S_x^2 - S_y^2$. As shown in Fig. 2, the correlations are weak and extremely short-ranged (~ 2 lattice constant). This indicates that the

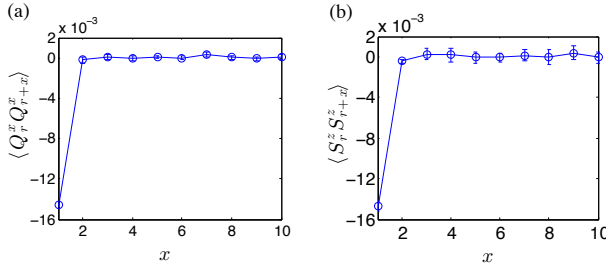


FIG. 2. (Color online) The correlation length on the bulk is extremely short, indicating the bulk is gapped and has no symmetry breaking.

bulk has a finite excitation gap and no symmetry breaking (otherwise the correlation will be long-ranged).

B. Trivial Topological Order

Here we check if the state $P_G|1-11\rangle$ has topological order by calculating its topological entanglement entropy (TEE) and ground state degeneracy.

TEE can be obtained from the second Renyi entropy $S^{(2)} = -\text{Tr}\rho_A^2$, which can be calculated using Monte Carlo method.⁴⁸⁻⁵² Suppose the system is divided into two parts A and B , ρ_A is the reduced density matrix of part A . For topologically ordered states, the entanglement entropy have an universal correction to the area law,

$$S^{(2)} = \alpha \mathbb{A} - \gamma,$$

where \mathbb{A} is the area of the boundary between A and B , and γ is called the topological entanglement entropy. If $P_G|1-11\rangle$ is a SPT state (which is short range entangled), its TEE γ should be zero.

This is checked numerically. We consider a torus and cut it along x direction to divide it into two pieces, each piece contains two non-contractable boundaries (see Fig. 3(b)). Area law suggest that the second Renyi entanglement entropy is proportional to the circumference of the cut (L_x). In Fig. 3(c), we fix $L_y = 10$ and plot the entropy with L_x . The TEE is given by the intersect, which is very close to 0. The inset shows the dependence of the TEE γ on L_y . The result is that γ exponentially decays to 0 with increasing L_y . The vanishing TEE implies that the state $P_G|1-11\rangle$ is indeed topologically trivial.

The trivial topological order carried by $P_G|1-11\rangle$ can also be reflected by its non-degeneracy on torus. As shown in Appendix C 1, the effective Lagrangian of the system can be described by

$$L_{\text{eff}} = i \frac{k}{2\pi} \dot{\theta}_x \theta_y, \quad (6)$$

where k is the degeneracy of ground states on torus and θ_x, θ_y are the gauge flux (or the angles of the gauge

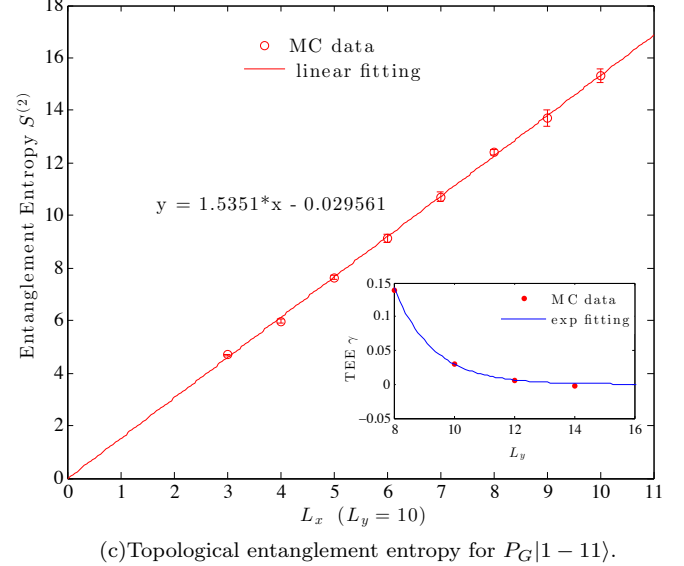
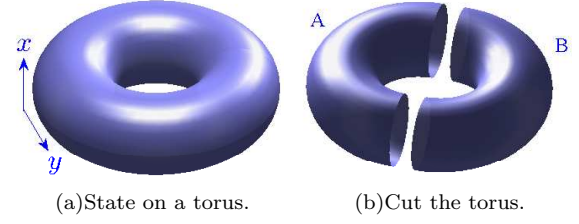


FIG. 3. Calculation of topological entanglement entropy (TEE) of state $P_G|1-11\rangle$ on a torus. (a) is the geometry of the torus and (b) shows how the torus is cut into the ‘system’ A and the ‘environment’ B . In (c), the second Renyi entanglement entropy $S^{(2)} = -\text{Tr}\rho_A^2$ is plotted VS the circumference L_x . The inset shows that γ exponentially decays to 0 with increasing ‘length’ L_y .

twist for the spinons) through x, y direction, respectively. Compactness of the internal gauge field indicates that $\theta_x \in [0, 2\pi], \theta_y \in [0, 2\pi]$. The Lagrangian (6) can be interpreted as the Berry phase of Gutzwiller projected states,

$$e^{-i \frac{k}{2\pi} \dot{\theta}_x \theta_y d\tau} = e^{-i \mathbf{A}(\boldsymbol{\theta}) \cdot d\boldsymbol{\theta}} = \langle P_G \psi_C(\boldsymbol{\theta}) | P_G \psi_C(\boldsymbol{\theta} + \delta\boldsymbol{\theta}) \rangle.$$

We can calculate the Chern number on the gauge twisted boundary condition space $k = \frac{1}{2\pi} \oint_B d\boldsymbol{\theta} \cdot \mathbf{A}(\boldsymbol{\theta}) = \frac{1}{2\pi} \iint_{\text{torus}} d\theta_x d\theta_y \mathcal{F}(\boldsymbol{\theta})$, where $\mathcal{F}(\boldsymbol{\theta}) = \partial_{\theta_x} \mathcal{A}_y - \partial_{\theta_y} \mathcal{A}_x$ is the Berry curvature and B is a big loop that encloses the total area of the torus. Our numerical result shows the Chern number of $P_G|1-11\rangle$ is 1, while the Chern number for the CSL state $P_G|111\rangle$ is 3, agreeing with theoretical prediction $k = \sum_m \mathcal{C}_m^{-1}$.

To verify that the ground state degeneracy is indeed equal to k , we calculate the density matrix of projected states with different twisted-boundary angles,

$$\rho(\boldsymbol{\theta}, \boldsymbol{\theta}') = \langle P_G \psi_C(\boldsymbol{\theta}) | P_G \psi_C(\boldsymbol{\theta}') \rangle. \quad (7)$$

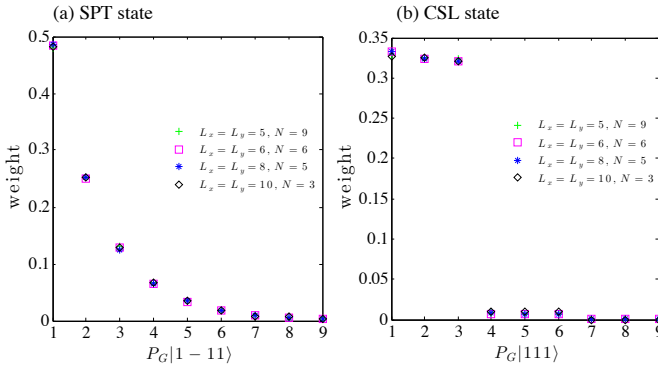


FIG. 4. (Color online) The biggest 9 (normalized) eigenvalues of the density matrix ρ are shown, which almost exhaust the total weight 1. (a) data for $P_G|1-11\rangle$; (b) data for $P_G|111\rangle$. The results are almost independent on the system size L_x, L_y (the number of sites is equal to $L_x \times L_y \times 3$) and the number of grids $N \times N$ by which the torus is discretized.

The eigen states of above density matrix are the orthonormal bases of the Hilbert space spanned by the projected states. In numerical calculation, the torus formed by $\theta_x \in [0, 2\pi]$ and $\theta_y \in [0, 2\pi]$ is discretized into $N \times N$ grids. Our result shows that the Hilbert space spanned by $\{|P_G\psi_C(\theta)\rangle\}$ is finite. The eigenvalues of ρ are proportional to the weights of the corresponding eigen-states in the GWF space. We can normalize the total weight to 1. Fig. 4 shows that the Hilbert space only contains very few number of bases (part of them are the ground states and the others are excited modes), and this result is independent on the system size and the number of grids on the (θ_x, θ_y) torus.

If one add a dynamic term $g(\dot{\theta}_x^2 + \dot{\theta}_y^2)$ (where g is non-universal) to Eq. (6), then it describes a single particle moving on a torus in an uniform magnetic field with strength k .⁴⁷ The eigen states are Landau levels and the lowest Landau level correspond to the ground state of the spin system. Higher Landau levels correspond to excited states and have relatively small weights. Since $|P_G\psi_C(\theta)\rangle$ is a superposition of several Landau levels, so there are some small weight eigenvalues appearing in Fig. 4. Furthermore, the degeneracy of eigenvalues of ρ reflects the degeneracy of the Landau levels, namely, the degeneracy of eigen states of the spin system. From Fig. 4(b), we can learn that all the eigenvalues of ρ for $P_G|111\rangle$ are 3-fold degenerate (within tolerable error), so the ground state is three-fold degenerate. However, for the state $P_G|1-11\rangle$, all the eigenvalues of ρ are non-degenerate, indicating that the ground state is unique.

C. Even-Quantized Hall conductance

We adopt Laughlin's gauge invariant argument on a cylinder to measure the Hall conductances. To this end, we adiabatically insert a $U(1)$ symmetry flux quanta ϕ^s

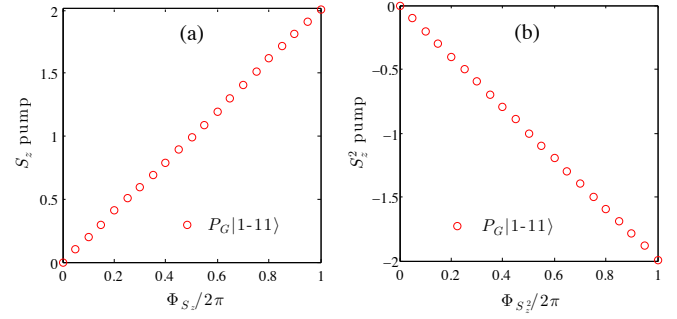


FIG. 5. (Color online) Symmetry charge pumping caused by inserting symmetry fluxes. The Hall conductance is equal to the charge pump by a flux quanta. (a) for the first $U(1)$ symmetry, the Hall conductance is equal to $\frac{1}{2\pi}2$; (b) for the second $U(1)$ symmetry, the Hall conductance is equal to $-\frac{1}{2\pi}2$.

into the cylinder and detect the $U(1)$ symmetry charge pumped from the bottom boundary to the top boundary. Since there are two $U(1)$ symmetries, we measure the Hall conductance respectively. During the measurement, we used the response mean field Hamiltonian (5) to obtain the GPWs. Our numerical results are shown in Fig. 5 where the Hall conductances are even integers, in consistent with Chern-Simons theory predictions.

The spin Hall conductance can also be calculated by measuring the Chern number of the projected states in $U(1)$ symmetry twisted boundary condition space (a torus). The Berry phase is calculated by the wave function overlap (see Appendix B) when adiabatically varying the symmetry fluxes through the two holes of the torus,

$$e^{-i\mathcal{A}(\phi_s)\delta\phi_s} = \langle P_G\psi_C(\phi_s, \bar{\phi}_g) | P_G\psi_C(\phi_s + \delta\phi_s, \bar{\phi}_g + \delta\phi_g) \rangle,$$

where $\psi_C(\phi_s, \bar{\phi}_g)$ is the mean field state with Chern numbers $\mathcal{C} = (\mathcal{C}_1 \mathcal{C}_0 \mathcal{C}_{-1})$, ϕ_s is the external symmetry flux and $\bar{\phi}_g$ is the induced internal gauge flux according to (4). Integration of the Berry curvature $\mathcal{F}(\phi_s) = \partial_{\phi_s^x} \mathcal{A}_y - \partial_{\phi_s^y} \mathcal{A}_x$ on the torus of (ϕ_s^x, ϕ_s^y) gives the Hall conductance

$$2\pi\sigma_{\text{SH}} = \oint_{\text{tourus}} d\phi_s^x d\phi_s^y \mathcal{F}(\phi_s) = \oint_B d\phi_s \cdot \mathcal{A}(\phi_s), \quad (8)$$

where B is a big loop that encloses the total area of the torus. Our numerical results confirms the spin Hall conductance shown in Fig. 5.

D. Symmetry protected Gapless boundary states

As mentioned, the spin-spin correlation function in the bulk is short ranged and boring. But the boundary is nontrivial. The nonzero Hall conductance indicates that the boundary should be gapless and the correlation function should be power law decaying. We would like to directly confirm the power law behavior for the boundary states. We calculate the correlation function $\langle Q^x(r)Q^x(r+x) \rangle$ (where $Q^x = S_x^2 - S_y^2$) on the boundary

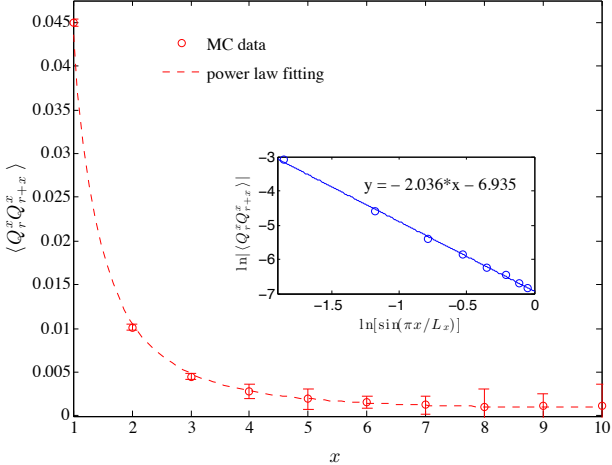


FIG. 6. (Color online) Power law decaying correlation function on the boundary (the upper boundary of Fig. 1a,b,c) shows that the edge states are gapless. The inset is a log-log fitting. The horizontal axis is set as $\ln(\sin \frac{\pi x}{L_x})$ because of finite size effect.

(along x direction) of a cylinder of 300 sites. The cylinder has $L_x \times L_y = 20 \times 5 = 100$ unit cells and is periodic in x direction and open in y direction (see Fig. 1b). The result shows perfect power (see Fig. 6),

$$\langle Q^x(r)Q^x(r+x) \rangle \sim x^{-2.036}$$

and the decaying power -2.036 agrees well with conformal field theory prediction -2 (see Appendix C2). It should be noted that the correlation function is very small even on the boundary. This may be owing to the extremely short correlation length on the bulk.

To completely confirm that $P_G|1-11\rangle$ is a SPT state, we finally need to show that its boundary state is non-chiral, namely, the gapless boundary excitations can be gapped out by symmetry breaking perturbations. Before projection, the mean field state $|1-11\rangle$ is obviously chiral and its boundary cannot be gapped out by small local perturbations. To show that the projected state $P_G|1-11\rangle$ is non-chiral, we calculate the boundary correlation function after adding some symmetry breaking perturbation.

The $U(1)$ symmetry breaking perturbation that we consider is the following fermion pairing term

$$H'_{\text{mf}} = \Delta_{ij}^1 c_{1i}^\dagger c_{1j}^\dagger + \Delta_{ij}^2 c_{-1i}^\dagger c_{0j}^\dagger + h.c. \quad (9)$$

The spin interaction that support this perturbation might be

$$H' = -(c_{1i}^\dagger c_{1j}^\dagger c_{-1j} c_{0i} + h.c.) = -(P_r^x Q_{r+x}^x - P_r^y Q_{r+x}^y),$$

where $P^x = \frac{1}{\sqrt{2}}(S_x S_z + S_z S_x + S_x S_y) = \begin{pmatrix} 0 & 1 & 0 \\ 1 & 0 & 0 \\ 0 & 0 & 0 \end{pmatrix}$, $P^y = \frac{1}{\sqrt{2}}(S_y S_z + S_z S_y + S_y S_x) = \begin{pmatrix} 0 & -i & 0 \\ i & 0 & 0 \\ 0 & 0 & 0 \end{pmatrix}$, and $Q^x = S_x^2 - S_y^2 =$

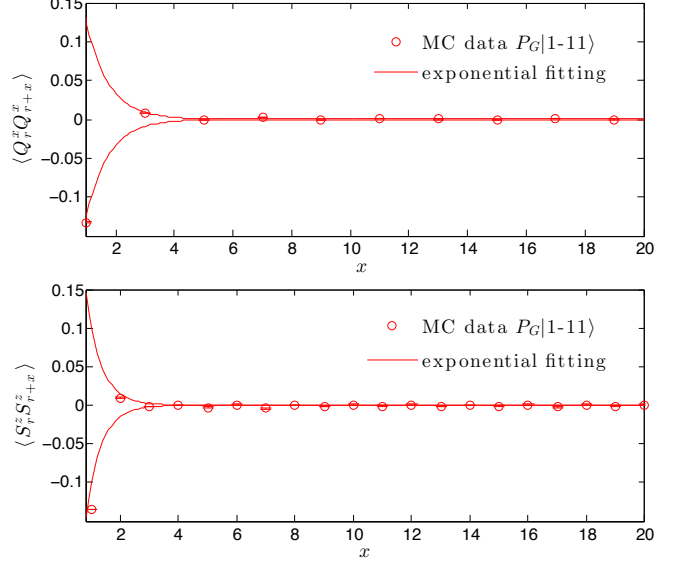


FIG. 7. (Color online) Boundary of SPT phase can be gapped when symmetry is explicitly broken.

$\begin{pmatrix} 0 & 0 & 1 \\ 0 & 0 & 0 \\ 1 & 0 & 0 \end{pmatrix}$, $Q^y = S_x S_y + S_y S_x = \begin{pmatrix} 0 & 0 & -i \\ 0 & 0 & 0 \\ i & 0 & 0 \end{pmatrix}$. Similar to S^x, S^y, S^z , the three operators Q^x, Q^y, S^z also form $SU(2)$ algebra.

Our numerical result is shown in Fig. 7, where the correlation function $\langle S_r^z S_{r+x}^z \rangle$ and $\langle Q_r^x Q_{r+x}^x \rangle$ are both exponentially decaying as expected.

We also calculate the boundary correlation function of the CSL undergoing the same perturbation. The results in Fig. 8 show that the boundary remains gapless under the perturbation. This comparison give strong evidence that the boundary of the state $P_G|1-11\rangle$ is non-chiral while the CSL state $P_G|111\rangle$ is chiral, as predicted by Chern-Simons theory (see Appendix C2).

IV. CONCLUSION AND DISCUSSION

In summary, using Monte Carlo method we studied the physical properties of Gutzwiller projected wave functions. We especially studied the state $P_G|1-11\rangle$ (where $1, -1, 1$ are the mean field Chern numbers of the fermions f_1, f_0, f_{-1} , respectively), including its spin Hall conductance, correlation function of the gapless edge states, ground state degeneracy and topological entanglement entropy, and non-robustness of the gapless edge states. All these evidence show that $P_G|1-11\rangle$ is a $U(1) \times U(1)$ symmetry protected topological state. Our work may shed some light on simple lattice models and experimental realization of SPT phases.

The spin Hall conductance is calculated by measuring the spin pump in the Gutzwiller wave function caused by inserting symmetry flux through the cylinder to the mean field Hamiltonian. We find that the internal gauge field

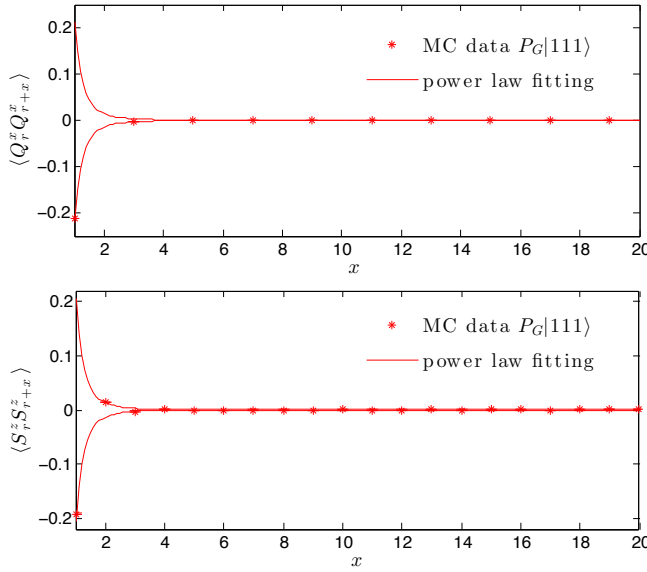


FIG. 8. (Color online) Boundary of CSL phase is robust against all perturbations.

plays an important role since external symmetry flux will induce a non-zero background internal gauge flux (see also Ref. 40). Our observation indicates that in general internal gauge field can not be ignored in studying physical response of Gutzwiller projected wave functions.

We also compared the SPT state $P_G|1-11\rangle$ with the topologically ordered chiral spin liquid state $P_G|111\rangle$ whose gapless boundary excitations are robust against all local perturbations. Our data imply that the boundary of the SPT state is non-chiral while the boundary of the chiral spin liquid is chiral. Noticing that at mean field level both $|1-11\rangle$ and $|111\rangle$ are chiral, it is remarkable that after Gutzwiller projection (or owing to strong interactions) the former becomes non-chiral. This indicates that physical properties of some mean field states might be dramatically changed after Gutzwiller projection.

Our Gutzwiller approach can be applied to study SPT states protected by other symmetry groups, such as $SU(2)$ or $SO(3)$ symmetry, and so on. It can be also used to study symmetry enriched topological phases, where symmetry interplays with topological order resulting in an enriched phase diagram.

We thank Y.-M. Lu, Y. Zhang, Z.-C. Gu, H. Yao, H.-H. Tu, M. Cheng, X.-L. Qi, C. Xu and P. A. Lee for helpful discussions. This research is supported in part by Perimeter Institute for Theoretical Physics. Research at Perimeter Institute is supported by the Government of Canada through Industry Canada and by the Province of Ontario through the Ministry of Economic Development & Innovation. ZXL thanks the support from NSFC 11204149 and Tsinghua University Initiative Scientific Research Program. XGW is also supported by NSF Grant No. DMR-1005541 NSFC 11274192, and the John Templeton Foundation.

Appendix A: Topological Entanglement Entropy

In Ref. 48–52, several tricks have been introduced to calculate Renyi entropy. The main trick is ‘sign trick’ which separates the calculation of the magnitude and phase of the swap operator:

$$e^{-S_2} = \langle \text{SWAP} \rangle = \sum_{\alpha_1 \alpha_2} \rho_{\alpha_1} \rho_{\alpha_2} \frac{\phi_{\beta_1} \phi_{\beta_2}}{\phi_{\alpha_1} \phi_{\alpha_2}} = \langle \text{SWAP} \rangle_{\text{amp}} \langle \text{SWAP} \rangle_{\text{phs}}, \quad (\text{A1})$$

where α_1, α_2 are the spin configurations of two independent systems of the same size, β_1, β_2 are the spin configurations after the swapping the spins in the holes, and

$$\langle \text{SWAP} \rangle_{\text{phs}} = \sum_{\alpha_1 \alpha_2} \tilde{\rho}_{\alpha_1, \alpha_2} e^{i\phi} \quad (\text{A2})$$

with $\phi = \text{Arg}(\phi_{\alpha_1}^* \phi_{\alpha_2}^* \phi_{\beta_1} \phi_{\beta_2})$ and $\tilde{\rho}_{\alpha_1, \alpha_2} = \frac{|\phi_{\alpha_1}^* \phi_{\alpha_2}^* \phi_{\beta_1} \phi_{\beta_2}|}{\langle \text{SWAP} \rangle_{\text{amp}}}$,

$$\begin{aligned} \langle \text{SWAP} \rangle_{\text{amp}} &= \sum_{\alpha_1, \alpha_2} |\phi_{\alpha_1}^* \phi_{\alpha_2}^* \phi_{\beta_1} \phi_{\beta_2}| \\ &= \sum_{\alpha_1, \alpha_2} \rho_{\alpha_1} \rho_{\alpha_2} \left| \frac{\phi_{\beta_1} \phi_{\beta_2}}{\phi_{\alpha_1} \phi_{\alpha_2}} \right| \end{aligned} \quad (\text{A3})$$

When calculating the phase part, since both the spin configurations before and after the swapping appear in the sampling weight, the trick of updating the inverse and determinant can be applied in the Monte Carlo steps. However, this trick can not be applied to the magnitude part since the swapped configuration may have zero weight and $\phi_{\beta_1}, \phi_{\beta_2}$ may not change continuously. To solve this problem and to decrease the error, here we further use the trick to separate the calculating the magnitude into two steps, in each step, the matrix inverse and determinant updating techniques can be applied. The main idea is to introduce a weight function $f(\alpha_1, \alpha_2)$:

$$f(\alpha_1, \alpha_2) = \begin{cases} 1, & \text{if } \beta_1, \beta_2 \text{ are allowed} \\ 0, & \text{if } \beta_1, \beta_2 \text{ are not allowed} \end{cases} \quad (\text{A4})$$

such that

$$\begin{aligned} \langle \text{SWAP} \rangle_{\text{amp}} &= \sum_{\alpha_1 \alpha_2} f(\alpha_1, \alpha_2) \rho_{\alpha_1} \rho_{\alpha_2} \left| \frac{\phi_{\beta_1} \phi_{\beta_2}}{\phi_{\alpha_1} \phi_{\alpha_2}} \right| \\ &= \sum_{\alpha_1 \alpha_2} \rho'(\alpha_1, \alpha_2) \left| \frac{\phi_{\beta_1} \phi_{\beta_2}}{\phi_{\alpha_1} \phi_{\alpha_2}} \right| \langle f(\alpha_1, \alpha_2) \rangle \\ &= \langle \text{SWAP} \rangle'_{\text{amp}} \langle f(\alpha_1, \alpha_2) \rangle \end{aligned} \quad (\text{A5})$$

where $\rho'(\alpha_1, \alpha_2) = \frac{f(\alpha_1, \alpha_2) \rho_{\alpha_1} \rho_{\alpha_2}}{\langle f(\alpha_1, \alpha_2) \rangle}$, and

$$\langle f(\alpha_1, \alpha_2) \rangle = \sum_{\alpha_1, \alpha_2} \rho_{\alpha_1} \rho_{\alpha_2} f(\alpha_1, \alpha_2).$$

Since $f(\alpha_1, \alpha_2)$ is a simple function taking values 0 and 1, the fluctuation is reduced considerably compared to $\langle \text{SWAP} \rangle_{\text{amp}}$ itself.

Appendix B: Overlap of wave functions

Suppose two normalized wave functions $|\psi_1\rangle$ and $|\psi_2\rangle$ are given as

$$|\psi_1\rangle = \sum_{\alpha} \frac{f_1(\alpha)}{\sqrt{\sum_{\beta} |f_1(\beta)|^2}} |\alpha\rangle,$$

$$|\psi_2\rangle = \sum_{\alpha} \frac{f_2(\alpha)}{\sqrt{\sum_{\beta} |f_2(\beta)|^2}} |\alpha\rangle,$$

where α means a spin configuration. To calculate the overlap between the two states $\langle\psi_1|\psi_2\rangle$, we introduce another normalized wave function $|\psi_0\rangle$ to generate the Monte Carlo sequence,

$$|\psi_0\rangle = \sum_{\alpha} \frac{h(\alpha)}{\sqrt{\sum_{\beta} |h(\beta)|^2}} |\alpha\rangle = \sum_{\alpha} W_{\alpha} |\alpha\rangle,$$

where $W_{\alpha} = \frac{h(\alpha)}{\sqrt{\sum_{\beta} |h(\beta)|^2}}$ is the weight of α .

Now we have

$$\begin{aligned} \langle\psi_1|\psi_2\rangle &= \sum_{\alpha} \frac{f_1^*(\alpha)f_2(\alpha)}{\sqrt{\sum_{\beta} |f_1(\beta)|^2 \sum_{\gamma} |f_2(\gamma)|^2}} \\ &= \sum_{\alpha} W_{\alpha} \frac{f_1^*(\alpha)f_2(\alpha)}{h^*(\alpha)h(\alpha)} \frac{\sum_{\sigma} |h(\sigma)|^2}{\sqrt{\sum_{\beta} |f_1(\beta)|^2 \sum_{\gamma} |f_2(\gamma)|^2}} \\ &= \frac{1}{C} \sum_{\alpha} W_{\alpha} \frac{f_1^*(\alpha)f_2(\alpha)}{h^*(\alpha)h(\alpha)}, \end{aligned} \quad (\text{B1})$$

where C is a constant:

$$\begin{aligned} C &= \sqrt{\frac{\sum_{\beta} |f_1(\beta)|^2 \sum_{\gamma} |f_2(\gamma)|^2}{\sum_{\sigma} |h(\sigma)|^2 \sum_{\delta} |h(\delta)|^2}} \\ &= \sqrt{\sum_{\beta} W_{\beta} \left| \frac{f_1(\beta)}{h(\beta)} \right|^2 \sum_{\gamma} W_{\gamma} \left| \frac{f_2(\gamma)}{h(\gamma)} \right|^2} \end{aligned} \quad (\text{B2})$$

Appendix C: Ground State Degeneracy and Boundary theory

1. Ground State Degeneracy

If we integrate out the $a_{m\mu}$ fields in the Chern-Simons action (3), we obtain

$$\mathcal{L}_{\text{eff}}(\tilde{a}) = \frac{i}{4\pi} k \varepsilon^{\mu\nu\lambda} \tilde{a}_{\mu} \partial_{\nu} \tilde{a}_{\lambda}, \quad (\text{C1})$$

where $k = \sum_m \mathcal{C}_m^{-1}$. If we further integrate out the \tilde{a}_0 field, we obtain a zero-strength condition

$$\partial_x \tilde{a}_y - \partial_y \tilde{a}_x = 0.$$

So we can write $\tilde{a}_i = \partial_i \Lambda + \theta_i / L_i$, where L_i is the size along i direction and θ_i can be interpreted as the angle

of twisted boundary condition for the fermionic spinons, or the gauge flux through the i th hole of the torus. Substituting above expression into (C1), we get the effective action

$$L_{\text{eff}} = \frac{i}{2\pi} k \dot{\theta}_x \theta_y, \quad (\text{C2})$$

which yields $[\theta_x, \frac{k}{2\pi} \theta_y] = i$. Define operators $T_i = e^{i\theta_i}$, then we have

$$T_x T_y = T_y T_x e^{i\frac{2\pi}{k}}, \quad (\text{C3})$$

which form a Heisenberg algebra.

Noticing \tilde{a}_0 is nothing but the chemical potential λ_i in (2), integrating out \tilde{a}_0 results in exactly one fermion per site, which is equivalent to a Gutzwiller projection. Eqn. (C2) shows that the GPW still have some degrees of freedom, which determines the ground state degeneracy.

The representation space of above Heisenberg algebra (C3) is at least k -dimensional. Since \tilde{a}_{μ} is a gauge degree of freedom for the original spin model, T_x and T_y will not change the spin Hamiltonian, namely, $[T_x, H] = [T_y, H] = 0$. So the Hilbert space of each energy level forms a representation space of the Heisenberg algebra. In other words, all the energy levels, including the ground state, are at least k -fold degenerate.

The degeneracy of the ground states can be obtained by calculating the Chern number for the Gutzwiller projected mean field states. At the mean field level, θ_x and θ_y are commuting, so we can construct mean field states with certain values of θ_x, θ_y , noted as $|\psi_{\mathcal{C}}(\theta_x, \theta_y)\rangle$, where \mathcal{C} denotes $(\mathcal{C}_1 \mathcal{C}_0 \mathcal{C}_{-1})$ for short. The topological term (C2) plays its role when \tilde{a}_0 is integrated out (or equivalently after Gutzwiller projection). If we interpret the topological term (C2) as the Berry phase of the Gutzwiller projected state evolving on the (θ_x, θ_y) torus,

$$\frac{k}{2\pi} \dot{\theta}_x \theta_y = i \langle P_G \psi_{\mathcal{C}}(\theta_x, \theta_y) | \partial_{\tau} | P_G \psi_{\mathcal{C}}(\theta_x, \theta_y) \rangle, \quad (\text{C4})$$

then k corresponds to the Chern number of the projected state,

$$2\pi k = \oint \frac{k}{2\pi} \dot{\theta}_x \theta_y d\tau = \oint_B d\boldsymbol{\theta} \cdot \boldsymbol{\mathcal{A}} \quad (\text{C5})$$

$$= \oint_{\text{torus}} d\theta_x d\theta_y \mathcal{F}(\boldsymbol{\theta}), \quad (\text{C6})$$

where $\boldsymbol{\mathcal{A}} = \langle P_G \psi_{\mathcal{C}}(\boldsymbol{\theta}) | i \partial_{\boldsymbol{\theta}} | P_G \psi_{\mathcal{C}}(\boldsymbol{\theta}) \rangle$ is the Berry connection (if θ_x, θ_y are discretized, then we have $e^{-i\boldsymbol{\mathcal{A}} \cdot \delta\boldsymbol{\theta}} = \langle P_G \psi_{\mathcal{C}}(\boldsymbol{\theta} + \delta\boldsymbol{\theta}) | P_G \psi_{\mathcal{C}}(\boldsymbol{\theta}) \rangle$) and $\mathcal{F}(\boldsymbol{\theta}) = \partial_{\theta_x} \mathcal{A}_y - \partial_{\theta_y} \mathcal{A}_x$ is the Berry curvature, B is the big loop enclosing the total area of the (θ_x, θ_y) torus.

Generally, the projected state $|P_G \psi_{\mathcal{C}}(\theta_x, \theta_y)\rangle$ is not an eigenstate of $T_i = e^{i\theta_i}$. In stead, an eigen state $|n_i\rangle$ of $T_i |n\rangle_i = e^{i2n\pi/k} |n\rangle_i$ (here $n = 0, 1, \dots, k-1$) is a superposition of $|P_G \psi_{\mathcal{C}}(\theta_x, \theta_y)\rangle$,

$$|n\rangle_i = \int d\theta_x d\theta_y \xi_{n_i}(\theta_x, \theta_y) |P_G \psi_{\mathcal{C}}(\theta_x, \theta_y)\rangle, \quad (\text{C7})$$

where $\xi_{n_i}(\theta_x, \theta_y)$ is a weight function in analog to a single particle wavefunction in the first Landau level.⁴⁷

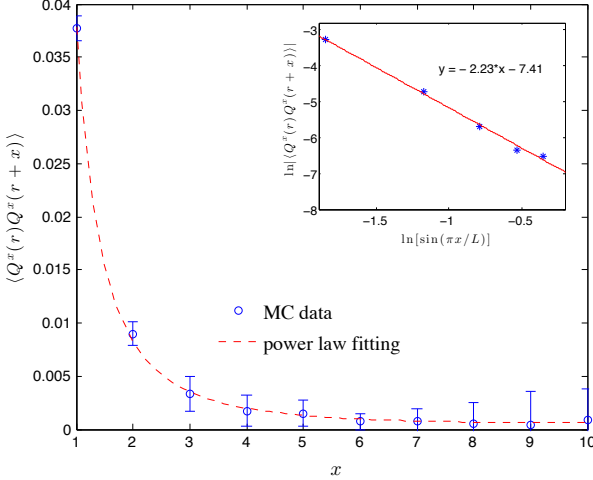


FIG. 9. (Color online) Correlation function of the boundary in an uniform Zeeman field $B_x = 0.4$. Power law decaying correlation function on the boundary shows that the edge states are still gapless. The inset is a log-log fitting, which shows that the decaying power is approximately -2.23 .

2. Boundary theory

In the remaining part, we will introduce an equivalent K -matrix description as the low energy effective theory. Integrating out the internal gauge field \tilde{a}_μ first, we obtain $\sum_m \partial_\nu a_{m\lambda} = 0$, or $\sum_m a_{m\lambda} = 0$ up to a constant field. Eliminating $a_{0\mu}$, we obtain the low energy effective Chern-Simons theory for the spin system,³⁷

$$\mathcal{L} = -\frac{i}{4\pi} \varepsilon^{\mu\nu\lambda} (a_{1\mu} \ a_{-1\mu}) K \partial_\nu \begin{pmatrix} a_{1\lambda} \\ a_{-1\lambda} \end{pmatrix} + \frac{i}{2\pi} \varepsilon^{\mu\nu\lambda} A_\mu^s (q_1 \ q_{-1}) \partial_\nu \begin{pmatrix} a_{1\lambda} \\ a_{-1\lambda} \end{pmatrix}, \quad (\text{C8})$$

where $K = \begin{pmatrix} \mathcal{C}_1^{-1} + \mathcal{C}_0^{-1} & \mathcal{C}_0^{-1} \\ \mathcal{C}_0^{-1} & \mathcal{C}_{-1}^{-1} + \mathcal{C}_0^{-1} \end{pmatrix}$, A_μ^s is the probing field according to some symmetry and $q = \begin{pmatrix} q_1 \\ q_{-1} \end{pmatrix}$ is the “charge vector” coupling to this probe field. For the $\sum_i S_i^z$ conservation symmetry, $q = \begin{pmatrix} 1 \\ -1 \end{pmatrix}$, while for the $\sum_i (S_i^z)^2$ conservation symmetry, $q = \begin{pmatrix} 1 \\ 1 \end{pmatrix}$. The Hall conductance is given by $\sigma_H = \frac{1}{2\pi} q^T K^{-1} q$.

Since (C8) is not gauge invariant if the system has a boundary, we need to introduce a boundary action to

recover the gauge invariance,

$$\mathcal{L}_{\text{boundary}} = -\frac{i}{4\pi} K_{IJ} \partial_\tau \phi_I \partial_x \phi_J - V_{IJ} \partial_x \phi_I \partial_x \phi_J, \quad (\text{C9})$$

where $I, J = 1, -1$, the field ϕ_I only exist on the boundary and is defined such that $a_{I\mu} = \partial_\mu \phi_I$. The ϕ_I field satisfy the Kac-Moody algebra

$$[\partial_x \phi_I, \partial_y \phi_J] = 2\pi i (K^{-1})_{IJ} \partial_x \delta(x - y). \quad (\text{C10})$$

The fermion operators can be written as $f_1 \sim e^{-i\phi_1}$, $f_{-1} \sim e^{-i\phi_{-1}}$. The spin density operator is given as $S_z \sim \partial_x \phi_1 - \partial_x \phi_{-1}$, and

$$Q^\pm = \frac{1}{2} (Q^x \pm iQ^y) \sim e^{i\phi_{\pm 1} - i\phi_{\mp 1}}. \quad (\text{C11})$$

If $\mathcal{C}_1 = 1, \mathcal{C}_0 = -1, \mathcal{C}_{-1} = 1$, then the K matrix is given as $K = \begin{pmatrix} 0 & -1 \\ -1 & 0 \end{pmatrix}$, from (C10) and (C11), we obtain the scaling law

$$\langle Q^+(r)Q^-(r+x) \rangle \sim x^{-2},$$

which is verified by the numerical result given in section III.

Furthermore, for above K matrix, since $l = \begin{pmatrix} n \\ 0 \end{pmatrix}$ or $l = \begin{pmatrix} 0 \\ n \end{pmatrix}$ (n is an integer) satisfies

$$l^T K^{-1} l = 0, \quad (\text{C12})$$

the Higgs term²⁴ that may gap out the boundary is $\cos(n\phi_1)$ or $\cos(n\phi_{-1})$. Eq. (C12) is the gapping condition for the perturbations. For instance, the pairing perturbation discussed in section III D satisfy the gapping condition. On the other hand, if this condition is not satisfied for some perturbation, for example, a Zeeman filed coupling

$$H' = B_x S_x \sim \cos(2\phi_1 + \phi_{-1}) + \cos(2\phi_{-1} + \phi_1)$$

which does not contain the Higgs term, then the boundary remains gapless even the symmetry is explicitly broken. This is verified by our numerical result shown in Fig. 9, where the correlation function $\langle Q^x(r)Q^x(r+x) \rangle$ remains power law if we add a Zeeman field $B_x = 0.4$ (in units of t_{ij}) to the whole system.

Finally, we give the Chern-Simons theory of the CSL state where $\mathcal{C}_1 = \mathcal{C}_0 = \mathcal{C}_{-1} = 1$. Form (C8), the K matrix of the CSL is given as $K = \begin{pmatrix} 2 & 1 \\ 1 & 2 \end{pmatrix}$. Since $\det K = 3$, The ground state degeneracy of CSL on a torus is 3. Furthermore, since there gapping condition (C12) has no solutions, the boundary can not be gapped out by small local perturbations.

¹ X. G. Wen, *Phys. Rev. B* **40**, 7387 (1989).

² X. G. Wen and Q. Niu, *Phys. Rev. B* **41**, 9377 (1990).

³ X. G. Wen, *International Journal of Modern Physics B* **04**, 239 (1990).

⁴ D. C. Tsui, H. L. Stormer, and A. C. Gossard, *Phys. Rev. Lett.* **48**, 1559 (1982).

⁵ R. B. Laughlin, *Phys. Rev. Lett.* **50**, 1395 (1983).

⁶ P. Anderson, *Materials Research Bulletin* **8**, 153 (1973).

⁷ P. W. Anderson, *Science* **235**, 1196 (1987).

⁸ L. D. Landau, *Phys. Z. Sowjetunion* **11**, 26 (1937).

⁹ V. L. Ginzburg and L. D. Landau, *Zh. Eksp. Teor. Fiz.* **20**, 1064 (1950).

¹⁰ X. Chen, Z.-C. Gu, and X.-G. Wen, *Phys. Rev. B* **82**, 155138 (2010).

¹¹ A. Kitaev and J. Preskill, *Phys. Rev. Lett.* **96**, 110404 (2006).

¹² M. Levin and X.-G. Wen, *Phys. Rev. Lett.* **96**, 110405 (2006).

¹³ Z.-C. Gu and X.-G. Wen, *Phys. Rev. B* **80**, 155131 (2009).

¹⁴ F. Pollmann, A. M. Turner, E. Berg, and M. Oshikawa, *Phys. Rev. B* **81**, 064439 (2010).

¹⁵ F. Haldane, *Physics Letters A* **93**, 464 (1983).

¹⁶ F. D. M. Haldane, *Physical Review Letters* **50**, 1153 (1983).

¹⁷ C. L. Kane and E. J. Mele, *Phys. Rev. Lett.* **95**, 146802 (2005), [cond-mat/0506581](#).

¹⁸ B. A. Bernevig and S.-C. Zhang, *Phys. Rev. Lett.* **96**, 106802 (2006).

¹⁹ J. E. Moore and L. Balents, *Phys. Rev. B* **75**, 121306 (2007), [cond-mat/0607314](#).

²⁰ L. Fu, C. L. Kane, and E. J. Mele, *Phys. Rev. Lett.* **98**, 106803 (2007), [cond-mat/0607699](#).

²¹ X.-L. Qi, T. Hughes, and S.-C. Zhang, *Phys. Rev. B* **78**, 195424 (2008), [arXiv:0802.3537](#).

²² X. Chen, Z.-C. Gu, Z.-X. Liu, and X.-G. Wen, *Phys. Rev. B* **87**, 155114 (2013).

²³ Z. Bi, A. Rasmussen, and C. Xu, [arXiv:1309.0515](#) (2013).

²⁴ Y.-M. Lu and A. Vishwanath, *Phys. Rev. B* **86**, 125119 (2012).

²⁵ X. Chen and X.-G. Wen, [arXiv:1206.3117](#) (2012).

²⁶ T. Senthil and M. Levin, *Phys. Rev. Lett.* **110**, 046801 (2013).

²⁷ N. Regnault and T. Senthil, *Phys. Rev. B* **88**, 161106 (2013).

²⁸ Z.-X. Liu and X.-G. Wen, *Phys. Rev. Lett.* **110**, 067205 (2013).

²⁹ X.-G. Wen, *Phys. Rev. B* **65**, 165113 (2002), [cond-mat/0107071](#).

³⁰ S.-P. Kou, M. Levin, and X.-G. Wen, *Phys. Rev. B* **78**, 155134 (2008), [arXiv:0803.2300](#).

³¹ S.-P. Kou and X.-G. Wen, *Phys. Rev. B* **80**, 224406 (2009), [arXiv:0907.4537](#).

³² A. Mesaros and Y. Ran, *Phys. Rev. B* **87**, 155115 (2013), [arXiv:1212.0835](#).

³³ L.-Y. Hung and Y. Wan, *Phys. Rev. B* **87**, 195103 (2013).

³⁴ Y.-M. Lu and A. Vishwanath, (2013), [arXiv:1302.2634](#).

³⁵ X. Chen, Z.-X. Liu, and X.-G. Wen, *Phys. Rev. B* **84**, 235141 (2011).

³⁶ M. Levin and Z.-C. Gu, *Phys. Rev. B* **86**, 115109 (2012).

³⁷ Y.-M. Lu and D.-H. Lee, [arXiv:1212.0863](#) (2013).

³⁸ P. Ye and X.-G. Wen, *Phys. Rev. B* **87**, 195128 (2013).

³⁹ Z.-X. Liu, Z.-C. Gu, and X.-G. Wen, [arXiv:1404.2818](#) (2013).

⁴⁰ J.-W. Mei and X.-G. Wen, [arXiv:1407.0869](#) (2014).

⁴¹ H.-H. Tu, A. E. Nielsen, and G. Sierra, *Nuclear Physics B* **886**, 328 (2014).

⁴² Z.-X. Liu, Y. Zhou, and T.-K. Ng, *Phys. Rev. B* **82**, 144422 (2010).

⁴³ Z.-X. Liu, Y. Zhou, and T.-K. Ng, *Phys. Rev. B* **81**, 224417 (2010).

⁴⁴ Z.-X. Liu, Y. Zhou, H.-H. Tu, X.-G. Wen, and T.-K. Ng, *Phys. Rev. B* **85**, 195144 (2012).

⁴⁵ S. Bieri, M. Serbyn, T. Senthil, and P. A. Lee, *Phys. Rev. B* **86**, 224409 (2012).

⁴⁶ This back ground internal gauge field \bar{a}_μ ensures that in the presence of probe field A_μ^s the net charge and current density still satisfy the number constraint. An alternative way to obtain (4) is integrating out the temporal component \bar{a}_0 which gives a constraint $\nabla \times \sum_m \mathcal{C}_m(\bar{\mathbf{a}} + q_m \mathbf{A}^s) = 0$. From the constraint, we can write $\bar{\mathbf{a}} = \bar{\mathbf{a}} + \delta\bar{\mathbf{a}}$, where $\bar{\mathbf{a}} = -\frac{\sum_m \mathcal{C}_m q_m}{\sum_m \mathcal{C}_m} \mathbf{A}^s$ (a background $\bar{a}_0 = -\frac{\sum_m \mathcal{C}_m q_m}{\sum_m \mathcal{C}_m} A_0^s$ is also induced owing to charge conservation) and $\delta\bar{\mathbf{a}}$ is locally a “pure gauge” since it satisfies $\nabla \times \delta\bar{\mathbf{a}} = 0$. As shown in section C 1, the term $\sum_m \mathcal{C}_m \epsilon_{\mu\nu\lambda} \delta a_\mu \partial_\nu \delta a_\lambda$ interprets the ground state degeneracy.

⁴⁷ X. G. Wen, *Phys. Rev. B* **40**, 7387 (1989).

⁴⁸ M. B. Hastings, I. González, A. B. Kallin, and R. G. Melko, *Phys. Rev. Lett.* **104**, 157201 (2010).

⁴⁹ J. I. Cirac and G. Sierra, *Phys. Rev. B* **81**, 104431 (2010).

⁵⁰ Y. Zhang, T. Grover, and A. Vishwanath, *Phys. Rev. Lett.* **107**, 067202 (2011).

⁵¹ Y. Zhang, T. Grover, and A. Vishwanath, *Phys. Rev. B* **84**, 075128 (2011).

⁵² J. Pei, S. Han, H. Liao, and T. Li, *Phys. Rev. B* **88**, 125135 (2013).